

## **Supporting Information**

### **Dual Metal Site–Mediated Efficient C–N Coupling toward Electrochemical Urea Synthesis**

Sourav Paul,<sup>a</sup> Sougata Sarkar,<sup>a</sup> Ashadul Adalder,<sup>a</sup> Amitava Banerjee,<sup>b</sup> and Uttam Kumar Ghorai\*<sup>a</sup>

- a. Swami Vivekananda Research Center, Ramakrishna Mission Vidyamandira, Belur Math, Howrah–711202, West Bengal, India.
- b. Department of Metallurgical and Materials Engineering, Indian Institute of Technology Jodhpur, Jodhpur, Rajasthan 342030, India

\*E-mail – [uttam.indchem@vidyamandira.ac.in](mailto:uttam.indchem@vidyamandira.ac.in)

## **Contents**

### **Experimental Section**

**SI 1:** Electrocatalyst ink preparation

**SI 2:** Determination of ammonia ( $\text{NH}_3$ )

**SI 3:** Determination of hydrazine ( $\text{N}_2\text{H}_4$ )

**SI 4:** Determination of  $\text{NO}_x$  contaminants

**SI 5:** Isotope labelling experiments by  $^1\text{H}$  NMR method

**SI 6:** Detection of urea using FTIR technique

**SI 7:** Density Functional Theory (DFT) Calculations

**SI 8:** Schematic representation of CoPc– $\text{MoS}_2$  synthesis process

**SI 9:** High Resolution XPS scan of ‘S’ in CoPc– $\text{MoS}_2$

**SI 10:** FTIR spectrum of CoPc– $\text{MoS}_2$

**SI 11:** UV–vis absorption spectra of different series concentrations of urea

**SI 12:** Calibration curve used for determination of urea concentration

**SI 13:** UV–vis absorption spectra of the electrolytes after electrocatalysis

**SI 14:** High resolution XPS spectra of the Co 2p after five cycles

**SI 15:** High resolution XPS spectra of the Mo 3d after five cycles

**SI 16:** High resolution XPS spectra of N1s after five cycles

**SI 17:** XRD pattern of CoPc– $\text{MoS}_2$  after electrolysis

**SI 18:** Time dependent current density (j) curves for CoPc at different potentials.

**SI 19:** Time dependent current density (j) curves for  $\text{MoS}_2$  at different potentials.

**SI 20:** UV–vis absorption spectra of the electrolytes at different potentials after 7200 s of electrocatalysis using CoPc.

**SI 21:** UV–vis absorption spectra of the electrolytes at different potentials after 7200 s of electrocatalysis using  $\text{MoS}_2$ .

**SI 22:** Urea yield rate with  $N_2$  and  $CO_2$  as feeding gas at different potentials for CoPc, CoPc–MoS<sub>2</sub> and MoS<sub>2</sub>.

**SI 23:** UV–vis absorption spectra of different ammonia concentrations

**SI 24:** Calibration curve used for determination of ammonia concentration

**SI 25:** Ammonia yield rate and FE at different potentials for CoPc–MoS<sub>2</sub>.

**SI 26:** UV–vis absorption spectra of different  $N_2H_4$  concentrations

**SI 27:** Calibration curve used for determination of  $N_2H_4$  concentration

**SI 28:** UV–vis absorption spectra for the formation of  $N_2H_4$  at different potentials.

**SI 29:** UV–vis absorption of CoPc–MoS<sub>2</sub> sample at  $-0.6$  V vs RHE in ( $N_2 + CO_2$ ) saturated, Ar saturated, and carbon paper in  $0.1$  M  $KHCO_3$  solution

**SI 30:** UV–vis absorption spectra of  $NO_x$  of various concentration solutions

**SI 31:** Calibration curve of  $NaNO_2$  with the given concentrations

**SI 32:** UV–vis absorption spectra for the formation of  $NO_x$  at  $-0.6$  V vs RHE

**SI 33.** Table: Comparison of the electrochemical urea performance for CoPc–MoS<sub>2</sub> with other electro-catalyst in solution media under ambient conditions.

**SI 34.** References

## Experimental Section

**Synthesis of Molybdenum sulfide:** MoS<sub>2</sub> nanosheets were synthesized by adding hexaammonium heptamolybdate tetrahydrate (0.25 mmol) and thiourea (0.5 mmol) to Millipore water, then mixing vigorously to form a homogeneous solution. Then, the solution is transferred Teflon-lined stainless steel autoclave and maintained at 200 °C for 20 h. The resultant product is washed with water and absolute ethanol several times to remove all unreacted molecules. Finally, the as-synthesized MoS<sub>2</sub> is dried at 60 °C under vacuum.

**Synthesis of CoPc–MoS<sub>2</sub> composite:** The MoS<sub>2</sub> was thoroughly exfoliated by ultra-sonication treatment for 48 hours in aqueous media, then centrifuged and dried in petri dish at 60 °C for 24 hours. Thereafter, 2.0 mg of MoS<sub>2</sub> nanosheets was collected by scraping with a surgical blade, and then it was dispersed in 20 mL water. In the solution 2 mg CoPc was added, and the dispersion was stirred for 20 hours. The composite was collected after centrifugation and dried under vacuum at 60 °C for 10 hours. The Fig. S1 shows the schematic representation of the synthesis of CoPc–MoS<sub>2</sub>.

**Characterizations Technique and Electrochemical Set-up:** Confirmation of Crystal structure and identification of phase of CuPc NTs were done by X-ray diffraction technique (XRD) using Bruker D-8 advanced Eco X-ray powder diffractometer instrument. A monochromatic radiation of Cu-K<sub>α</sub> (wavelength,  $\lambda=0.15404$  nm) was used in X-ray diffraction technique and the ideal equilibrium conditions were maintained by using voltage of 40 kV and a current of 25 mA respectively. The amount of urea was quantified by making the use of UV-vis spectrophotometer (Shimadzu, UV-3600 plus). All the measurements involving electro-catalytic reduction of N<sub>2</sub> and CO<sub>2</sub> were done using a CHI 760E electrochemical instrument which was comprised of a three-electrode system containing a

platinum (Pt) wire acting as counter electrode and Ag/AgCl (in 3.5 M KCl) acting as the reference electrode and carbon paper loaded with CuPc catalyst ink acting as the working electrode. All the readings of potential were correctly transformed with respect to that of the reversible hydrogen electrode (RHE). All electrochemical process was carried out in an H-type cell.

**Determination of Urea:** The urea quantification was carried out by UV-vis spectrophotometer utilizing the diacetyl monoxime (DAMO) method. The intensity of absorbance of the colored solution will have a directly proportionality relationship with the concentration of urea. Color reagents required for this procedure (solution A and solution B) were prepared following the process described below:

Preparation of solution A (acid ferric solution): conc.  $\text{H}_2\text{SO}_4$  (30 ml) (Merck) and conc. phosphoric acid (Sigma-Aldrich) (10 ml) were mixed with triple distilled water (Millipore) (60 ml). Then 10 mg ferric chloride was added to the solution.

Preparation of solution B (DAMO-TSC solution): diacetyl monoxime (DAMO) (Sigma-Aldrich) (weighted 0.25 g) and thiosemicarbazide (TSC) (Sigma-Aldrich) (weighted 5 mg) were dissolved homogeneously in triple distilled water (50 ml). A concentration series of urea (0.0, 0.2, 0.4, 0.6, 0.8, and 1.0  $\mu\text{g}\cdot\text{ml}^{-1}$ ) were prepared for standard calibration purpose. Sequentially, 2 ml of solutions A and 1 ml of solution B were mixed with the concentration series solution(s) of urea and each of the resulting solution were shaken vigorously. Then each of the resulting solution was heated at 100°C for the certain time period until the generation of pink colored solution. The pink colored solutions were cooled to room temperature and absorbance of the solutions was measured by UV-vis spectroscopy technique. It was noted from literature survey that the maxima of absorbance peak come at 525 nm. [1] The

absorbance curve led to the standard calibration with the linear relation ( $y = 0.1515 x + 0.077$ ,  $R^2 = 0.9994$ ).

**Calculation of the Urea Yield Rate and Faradaic Efficiency:** After electrochemical co-reduction of  $N_2$  and  $CO_2$  to urea, the urea yield rate and Faradaic efficiency were calculated by the given equation:

$$\text{Urea yield rate} = \frac{(C_{\text{urea}} \times V)}{(m_{\text{cat}} \times t)} \dots\dots\dots(1)$$

$$\text{FE (\%)} = \frac{(6 \times F \times C_{\text{urea}} \times V)}{(60.06 \times Q)} \times 100\% \dots\dots\dots(2)$$

Where,  $C_{\text{urea}}$  is concentration of urea produced after electrochemical co-reduction of  $N_2$  and  $CO_2$ ,  $V$  is the total volume of electrolyte taken,  $t$  is the time required for co-reduction of gases,  $m$  is the catalyst mass,  $F$  is the Faradaic constant ( $96,485 \text{ C mol}^{-1}$ ) and  $Q$  is the total charge passing through the electrode.

**SI 1: Electrocatalyst ink preparation:** 1.2 mg CoPc–MoS<sub>2</sub> catalyst was precisely weighed and dispersed with 250 μL 2-propanol (Merck) solution. The solution was sonicated for few seconds to make a uniform dispersion. Further, 20 μL Nafion 117 (5wt %) (Sigma-Aldrich) solution was added to the dispersion to play the role of binder. Finally, the prepared dispersion was agitated for a minute to turn it into a homogeneous and useable catalytic ink for further use. 40 μL of the prepared ink was loaded on a 1 x 1cm<sup>2</sup> carbon paper substrate.

**SI 2: Determination of ammonia (NH<sub>3</sub>):** The indophenol blue test was used for quantitative measurement of the ammonia produced during electrochemical process. For calibration purpose, ammonium sulphate (Merck Co., Ltd.) solutions of different concentration {1.0, 0.8, 0.6, 0.4, 0.2, 0.0 (μg mL<sup>-1</sup>)}(To be changed) in 0.1 molar KHCO<sub>3</sub> solution were prepared, then plot was obtained demonstrating the relation of concentration and absorbance. The supplementary **Figure S15** shows a linear relationship between absorbance and concentration with the fitting curve ( $y = 0.15414 x + 0.03443$ ;  $R^2 = 0.9984$ ). The results were reported after the experiments were performed for three times to ensure reproducibility.

$$\text{Ammonia yield rate} = \frac{(C_{\text{NH}_3} \times V)}{(m_{\text{cat}} \times t)} \dots\dots\dots (1)$$

Where ‘C<sub>NH<sub>3</sub></sub>’ is concentration of ammonia produced electrocatalytically, ‘V’ is electrolyte volume, ‘t’ is time of electrochemical reduction reaction and ‘m’ is loaded mass of the catalyst on the working electrode.

$$\text{FE (NH}_3) = \frac{(3 \times F \times C_{\text{NH}_3} \times V)}{(M \times Q)} \times 100\% \dots\dots\dots (2)$$

Where 'F' is the Faraday Constant, ' $C_{\text{NH}_3}$ ' is concentration of ammonia; 'V' is volume of the electrolyte, 'M' is the molecular mass of ammonia, 'Q' is the total charge passed through the electrode during the electrolysis.

**SI 3: Determination of hydrazine ( $\text{N}_2\text{H}_4$ ):** To detect the hydrazine if produced during electroreduction of  $\text{N}_2$  and  $\text{CO}_2$ , Watt and Chrisp process was utilized. [2] In detail, the colorant was prepared with 5.99 g of para-(dimethylamino) benzaldehyde (Merck), 30 ml concentrated HCl (Merck), and 300 ml ethanol (Merck). After the dual gas electroreduction, 5 ml of electrolyte solution was taken and added to 5 ml of colorant solution and then agitated for 15 minutes and incubated in a dark place at standard temperature for another 5 minutes, after a while the absorption spectrum of the solution was noted. The maximum absorption was observed at 455 nm (**Figure S17**). The calibration series was prepared in the following way: Initially, a series of different concentration of hydrazine-monohydrate was made as standard solution (0.0, 0.2, 0.4, 0.6, 0.8, and 1.0  $\mu\text{g mL}^{-1}$ ) in 0.1 M  $\text{KHCO}_3$  solution. The volume was then adjusted to 5 ml using 0.1 M  $\text{KHCO}_3$  solution. The prepared hydrazine-hydrate solution was then added to 5 ml of colorant solution and stirred at room temperature for 10 minutes and after stirring, the solution was incubated at a dark place at room temperature for 10 minutes; The UV-visible spectrum was then tested and the maximum absorption peak was observed 460 nm. The plot of absorption and concentration curve (**Figure S18**) resulted into a fitting plot ( $y = 0.7971 x - 0.0019$ ;  $R^2 = 0.999$ ). The absorption and concentration curve displayed a linear relationship in between them, then after three distinct calibrations it was reported for the hydrazine estimate. It was shown that there is no hydrazine produced after the co-reduction of  $\text{N}_2$  and  $\text{CO}_2$  at different potential (**Figure S19**).

**SI 4: Determination of NO<sub>x</sub> contaminants:** The quantitative estimation of NO<sub>x</sub> was carried out using *N*-(1-naphthyl)-ethylene diamine dihydrochloride. The colorant solution was made by dissolving 0.5 g of sulfanilic acid (Merck), 5 ml acetic acid (Merck) and 5 mg of *N*-(1-naphthyl)-ethylene diamine dihydrochloride (LobaChemie) into 95 ml of millipore water. Then, 1 ml of electrolyte was added to 4 ml of dye solution. Then, after incubating for 15 minutes, an absorption spectrum was obtained using an ultraviolet-visible spectrophotometer. The calibration curves were plotted using sodium nitrite (Merck) solution at a range of concentrations in 0.1 M KHCO<sub>3</sub>. The plot of absorption vs concentration (**Figure S22**), generates a fitting plot ( $y = 0.20166x + 0.01064$ ;  $R^2 = 0.999$ ) showing a linear relationship of absorbance and concentration of NO<sub>x</sub>. We conclude from (**Figure S23**), the UV-vis absorption spectra of 0.1 M KHCO<sub>3</sub> background and ultra-high purity (99.999% purity) N<sub>2</sub> and CO<sub>2</sub> (99.99% purity) gas flushed electrolyte that NO<sub>x</sub> was not present in the feeding gas. Thus, it is confirmed that urea is formed by reducing the supplied N<sub>2</sub> and CO<sub>2</sub> gas.

**SI 5: Isotope labelling experiments by <sup>1</sup>H NMR method:** The isotope tracing experiment was done using dual gas system; <sup>15</sup>N<sub>2</sub> (98 atom% <sup>15</sup>N Sigma-Aldrich Co.) and <sup>12</sup>CO<sub>2</sub> (99.999% ultra-high purity grade) were used to saturate the electrolyte solution to verify the origin of urea formation. After close to 20 hours of simultaneous co-reduction of N<sub>2</sub> and CO<sub>2</sub> gases at a potential of -0.7 V (vs. RHE), the subjected electrolyte was concentrated using a distillation process. Then the concentrated electrolyte solution was used to test the formation of urea by <sup>1</sup>H-NMR method (Bruker 600 MHz, USA) by using an internal standard of d<sup>6</sup>-DMSO (Cambridge Isotope Laboratories Inc.). The NMR spectrum was obtained after 6 hours run with 2000 scans.

**SI 6: Detection of urea using FTIR technique:** The chemical bonds formed during the electrocatalytic urea synthesis process was characterized using in situ ATR–FTIR technique. After two hours of electrocatalytic co–reduction process, the 1  $\mu\text{L}$  electrolyte solution was drop at the tip of the diamond present in the ATR mode in the FTIR instrument. The FTIR measurements for the different potentials were made with the background scans using 1  $\mu\text{L}$  0.1 M  $\text{KHCO}_3$  solution. The specifications of the FTIR instrument parameters to conduct the experiment are as follows: wavelength range from  $4000\text{ cm}^{-1}$  –  $400\text{ cm}^{-1}$ , 50 number of scans, mirror speed of 2.8, maximum resolution were set using standard detector.

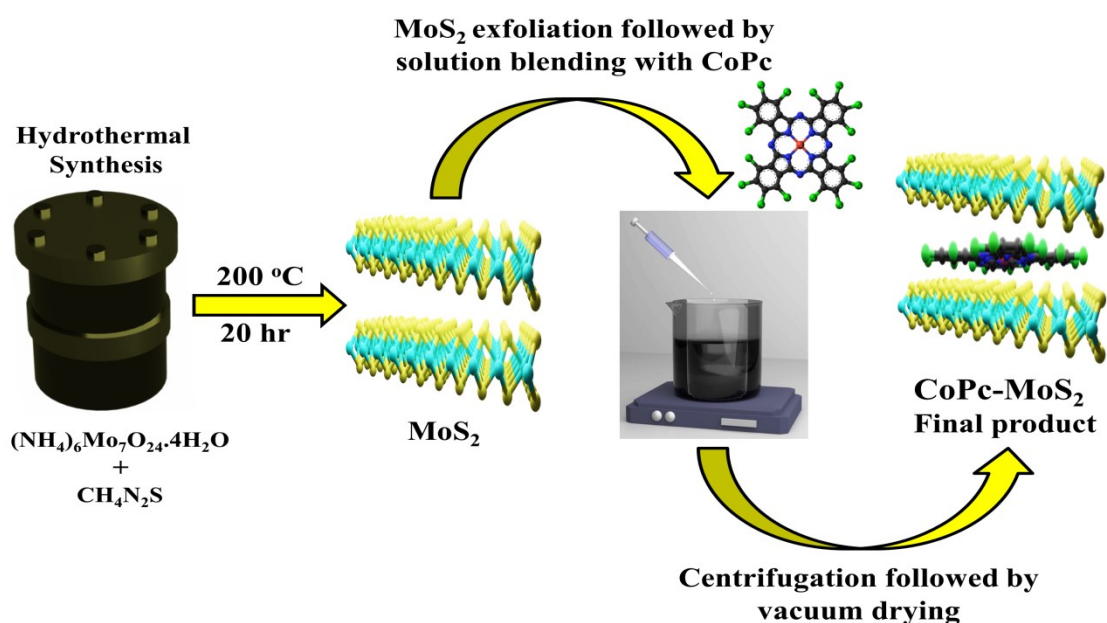
**SI 7: Density Functional Theory (DFT) calculations:**

DFT spin-polarized calculations were performed using the projector-augmented wave (PAW) method [3] implemented in the Vienna Ab-initio Simulation Package (VASP) [4,5]. For exchange-correlation potential, we employed generalized gradient approximation (GGA) in Perdew-Burke-Ernzerhof (PBE) formalism. A vacuum space of over 20 Å is considered along the Z-direction of the Mo terminated surface to avoid interactions between periodic images. To account for van der Waals interactions, important for hydrogen adsorption energies estimation, we used the DFT-D3 approach [6] throughout all calculations. Ground state geometries of large supercell were obtained with  $1 \times 1 \times 1$  Monkhorst-Pack set of k-points, the force convergence criteria of  $10^{-3}\text{ eV/\AA}$  and the total energy convergence criteria in the self-consistent field iteration of  $10^{-6}\text{ eV}$ . The plane-wave basis set cut-off was 520 eV. With this set of parameters, the numerical precision of adsorption energies calculations is meV. Pseudopotentials is constructed by the PAW method, which treats the following electrons as valence: 1s for H,  $2s^2 2p^3$  for N,  $3s^2 3p^4$  for S,  $3p^6 3d^8 4s^1$  for Co  $4p^6 4d^5 5s^1$  for Mo and  $2s^2 2p^2$  for C. Geometry relaxation was performed by conjugate-gradient method. Bader charge density analysis [7] was performed to calculate the atomic charges.

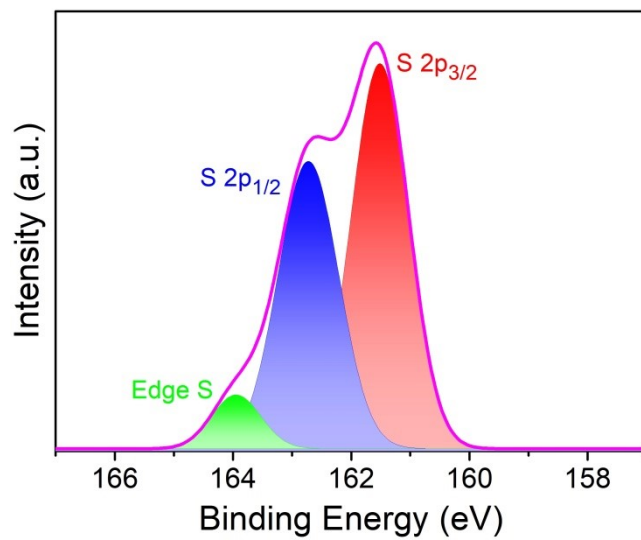
During the urea formation, processes without proton coupling and with net proton-coupling and electron transfer takes place. In the later cases, the electron–proton pairs in the solution ( $H^+ + e^-$ ) are gradually added to the intermediates, CONN. The change in Gibbs free energy ( $\Delta G$ ) of each step is calculated according to the computational hydrogen electrode (CHE) model, and chemical potential of electron–proton pair is half that of hydrogen, i.e.,  $H^+ + e^- \rightleftharpoons 1/2 H_2$  [8]. In this model, a standard vibrational correction method is used in the harmonic approximation to the enthalpy, and entropy is also used for correcting the free energy to the electronic energy:  $\Delta G = \Delta E + \Delta ZPE - T\Delta S + \Delta G_U$ , where  $\Delta E$  is the difference of the electronic energy directly obtained from DFT calculation results,  $T$  is the temperature ( $T = 298.15$  K),  $\Delta ZPE$  is the zero-point energy,  $\Delta S$  is the change of the entropy, and  $\Delta G_U$  is the contribution of free energy related to the applied electrode potential  $U$ . The free energy profiles in this study haven't considered any other  $U$  except  $U=0$ . Notably, the entropies and zero-point energies of these intermediate species for electrochemical urea synthesis were obtained by DFT calculations.

**Bader charge analysis:** DFT based electronic structure and Bader charge analysis has been carried out to further understand the insight of the  $N_2$  activation process. We have considered various possibilities of  $N_2$  adsorption sites, where we have the possibilities of single transition metal activation and double transition metal activation. Bader charge analysis depicts that the surface Mo atom which is bonded with  $N_2$  has net Bader charge 1.076 e ( whereas the surface Mo atoms which are not bonded with  $N_2$  has Bader charge  $\sim 0.734$  e). This is showing that Mo is transferring charge to  $N_2$ . Co (whose net bader charge is 1.083 e) of CoPC is also transferring charge to  $N_2$ . Net Bader charge of N bonded with Co is  $-0.238$  and N bonded with Mo is  $-0.478$ .

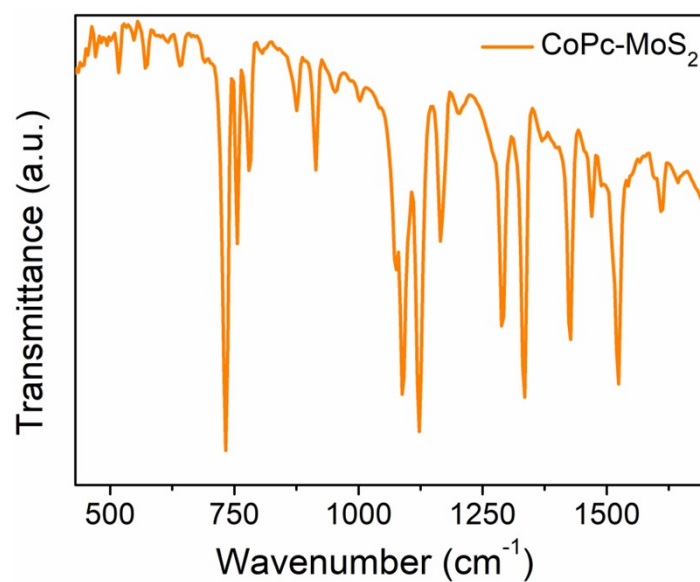
**Density of State analysis (DOS):** DOS has shown that the Fermi region is dominated by the Mo\_d and S\_p orbitals along with nominal contribution from other elements. A strong hybridization of transition metal orbitals with the adsorbed N<sub>2</sub> also indicates the possibility of sharing the charge back and forth with the adsorbed N<sub>2</sub>, as observed in the Bader charge analysis.



**Figure S1.** Schematic representation of CoPc-MoS<sub>2</sub> synthesis



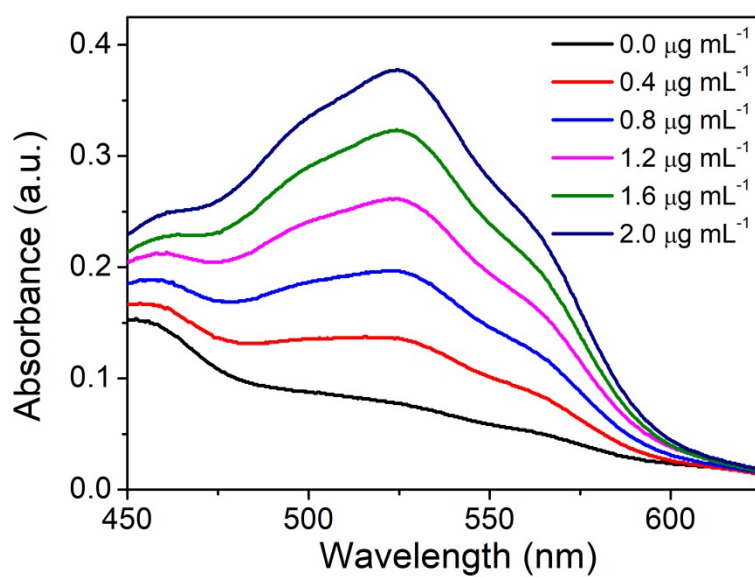
**Figure S2:** High resolution XPS survey scan of the S 2p in CoPc-MoS<sub>2</sub>



**Figure S3.** FTIR spectrum of CoPc-MoS<sub>2</sub>

**Table S1:** FTIR bonding analysis of CoPc–MoS<sub>2</sub> [9–13]

Wavenumber (cm <sup>-1</sup> )	Assigned bonds
472 cm <sup>-1</sup>	S–S bond deformation
646 cm <sup>-1</sup>	S–S bond stretching
755 cm <sup>-1</sup>	Co–N bond vibration
781 cm <sup>-1</sup>	C=N in plane stretching vibration
877, 1427, 1622 cm <sup>-1</sup>	Attributed to MoS <sub>2</sub>
1088 cm <sup>-1</sup>	C–H in plane deformation
1123 cm <sup>-1</sup>	Isoindole total symm.
1165 cm <sup>-1</sup>	δ C–N in plane deformation + isoindole
1289 cm <sup>-1</sup>	C–H in plane deformation
1334 cm <sup>-1</sup>	C–N stretching in isoindole
1469 cm <sup>-1</sup>	C–C stretching in Isoindole
1522 cm <sup>-1</sup>	C=N stretching

**Figure S4:** UV–vis absorption spectra of different series concentrations of urea

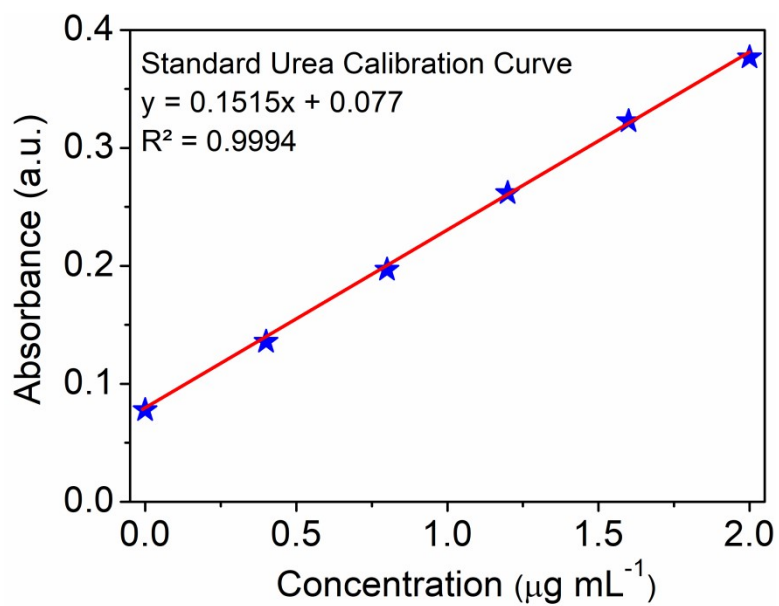


**Figure S5:** Calibration curve used for determination of urea concentration

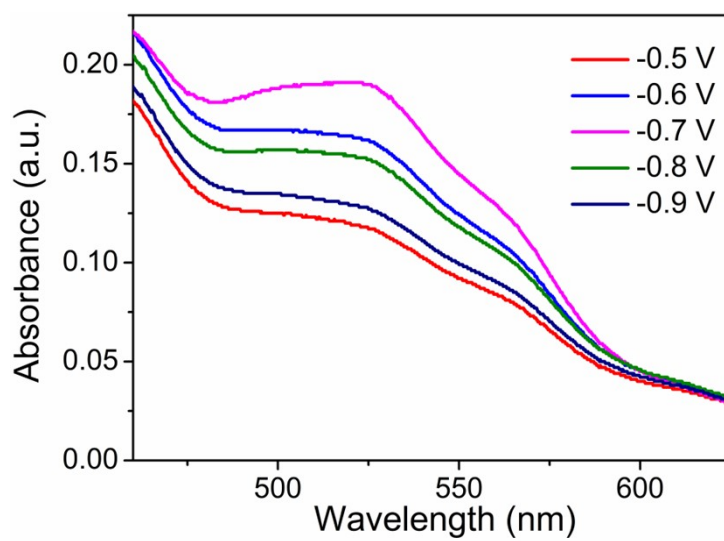


**Figure S6:** UV-vis absorption spectra of the electrolytes at different potentials after 7200 s of electrocatalysis.

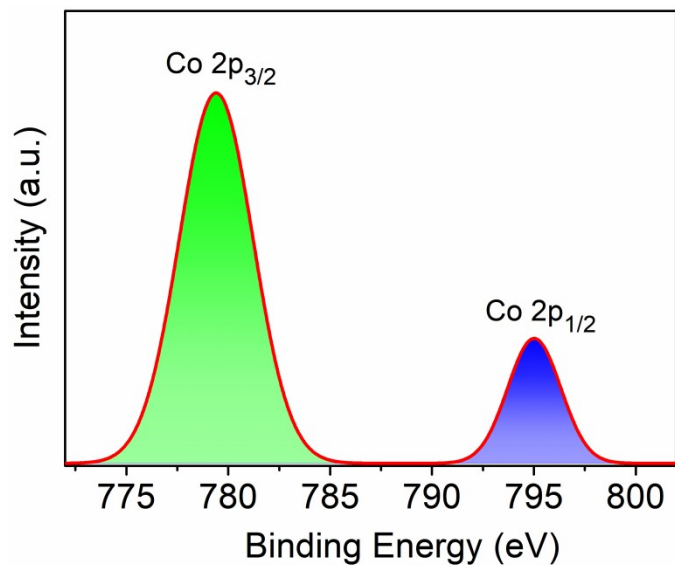


**Figure S7:** High resolution XPS spectrum of Co 2p doublet in CoPc–MoS<sub>2</sub> after five cycles

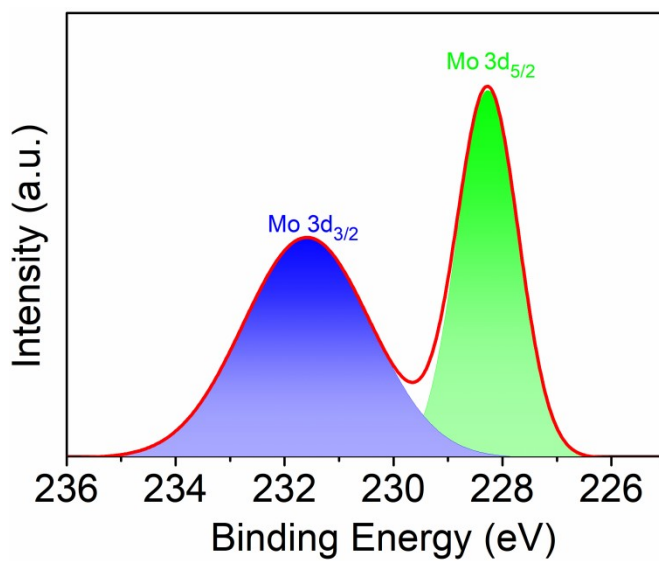


**Figure S8:** High resolution XPS spectra of the Mo 3d in CoPc–MoS<sub>2</sub> after five cycles

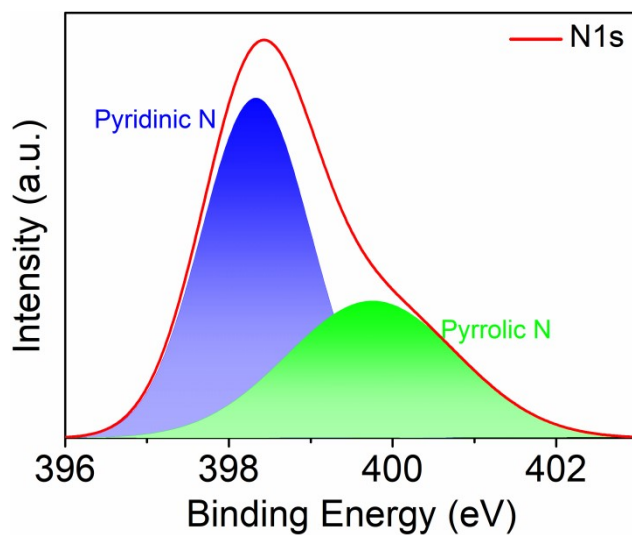


**Figure S9:** High resolution XPS spectra of the N 1s after five cycles

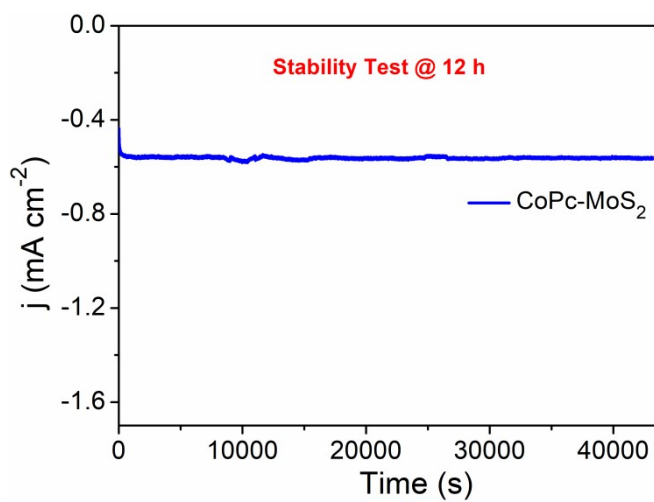


**Figure S10:** Time dependent current density ( $j$ ) curves for CoPc-MoS<sub>2</sub> at  $-0.7$  V vs. RHE after 12 h electrocatalysis.

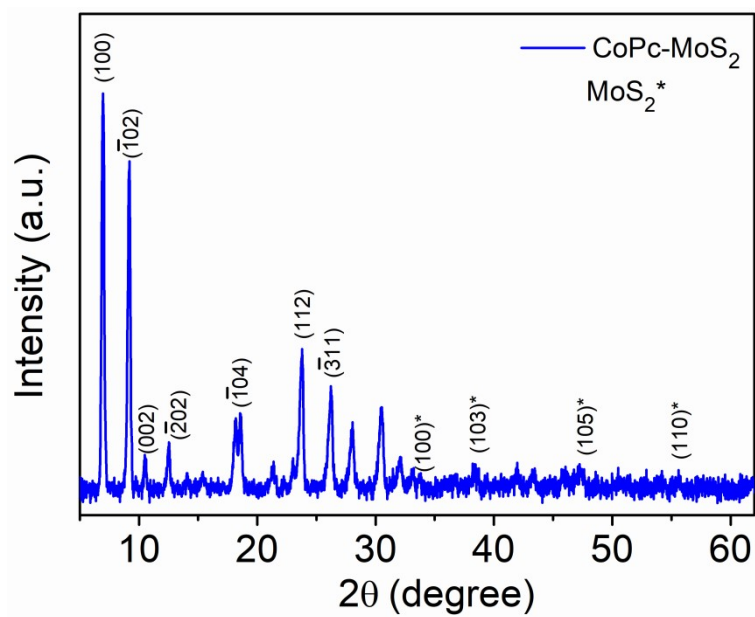


**Figure S11:** XRD pattern of CoPc–MoS<sub>2</sub> after electrolysis

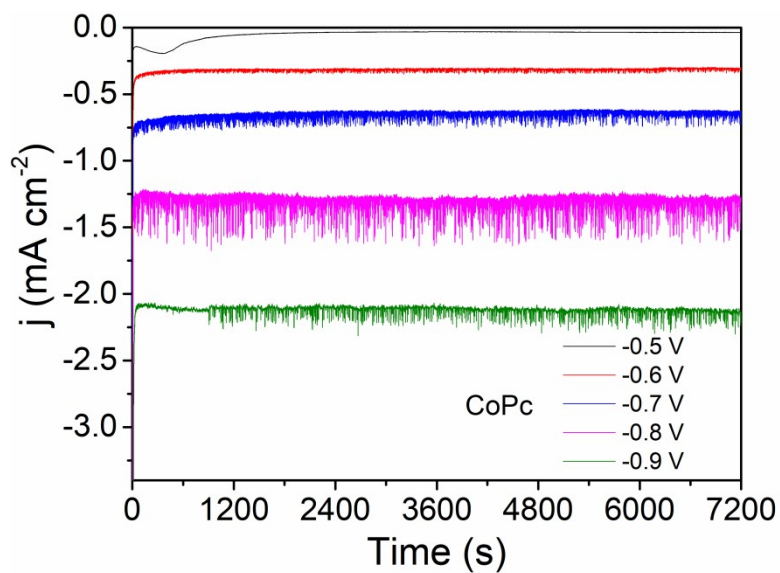


**Figure S12:** Time dependent current density ( $j$ ) curves for CoPc at different potentials.

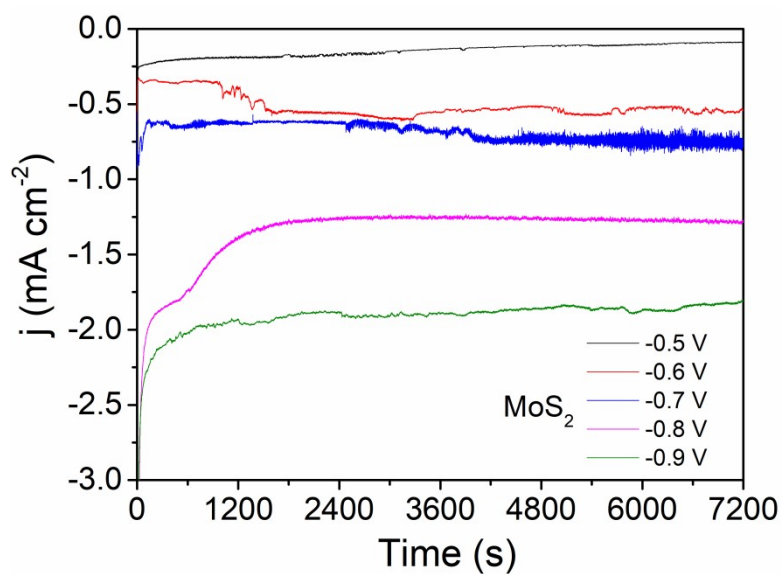


**Figure S13:** Time dependent current density ( $j$ ) curves for  $\text{MoS}_2$  at different potentials.

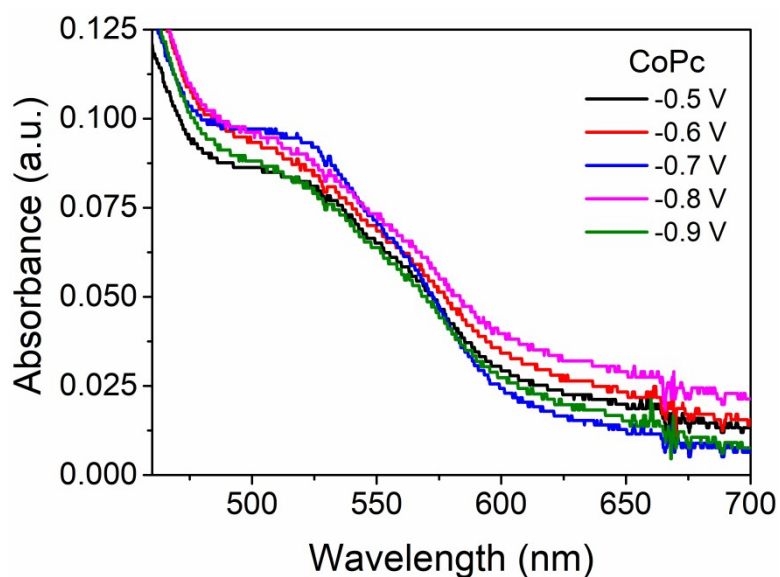


**Figure S14:** UV-vis absorption spectra of the electrolytes at different potentials after 7200 s of electrocatalysis using CoPc.

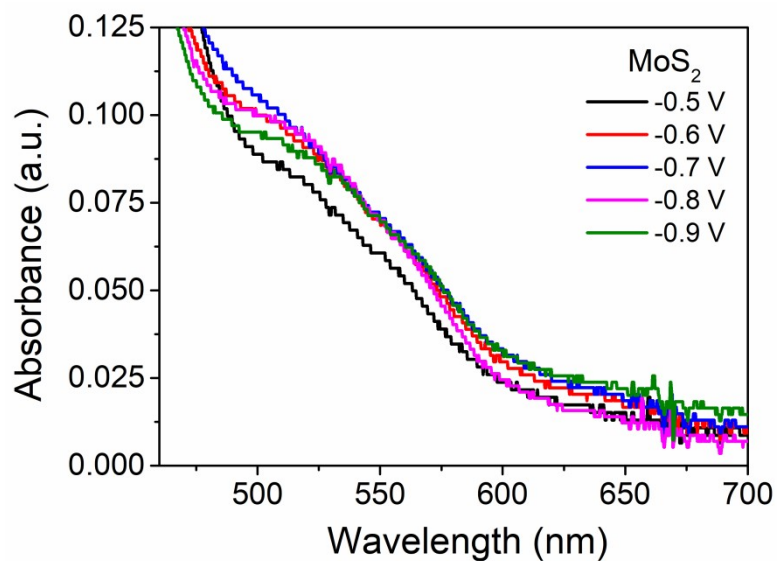


**Figure S15:** UV-vis absorption spectra of the electrolytes at different potentials after 7200 s of electrocatalysis using MoS<sub>2</sub>.

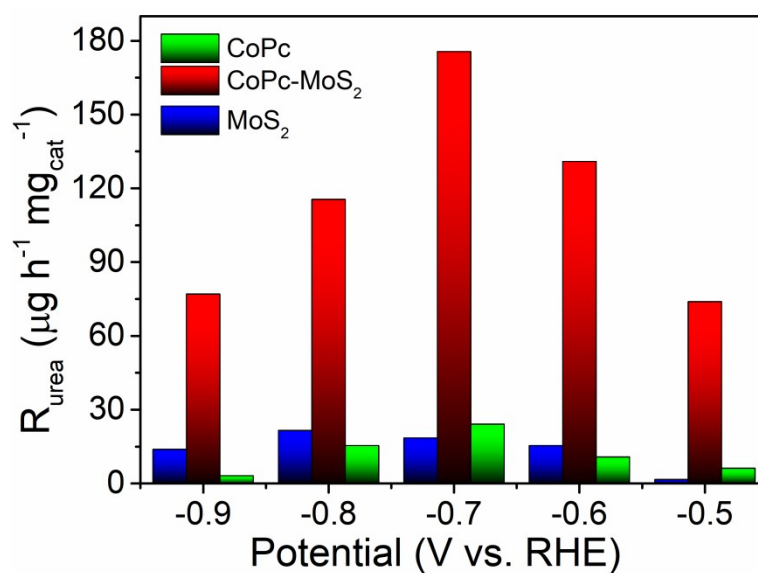


**Figure S16:** Urea yield rate with N<sub>2</sub> and CO<sub>2</sub> as feeding gas at different potentials for CoPc, CoPc-MoS<sub>2</sub> and MoS<sub>2</sub>.

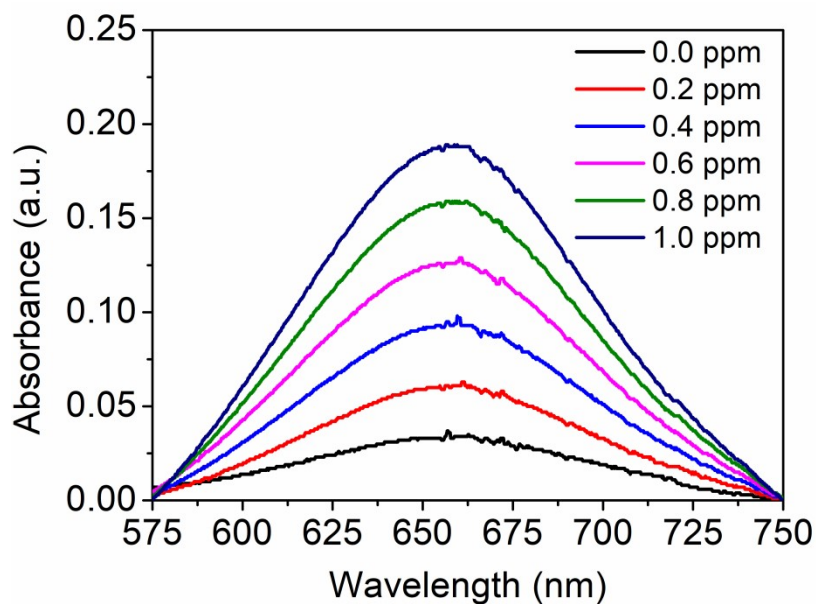


**Figure S17:** UV-vis absorption spectra of various ammonia concentrations

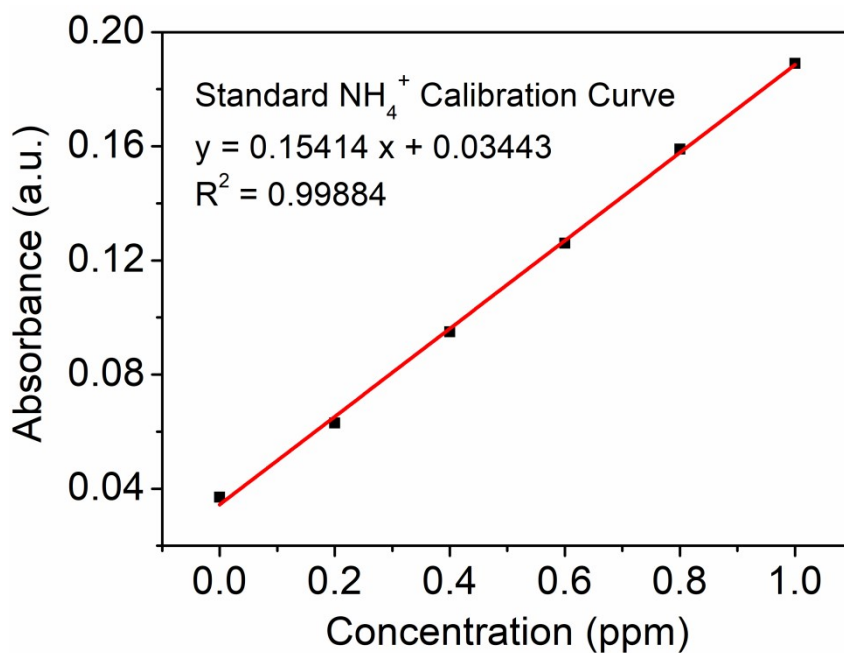


**Figure S18:** Calibration curve used for determination of ammonia concentration

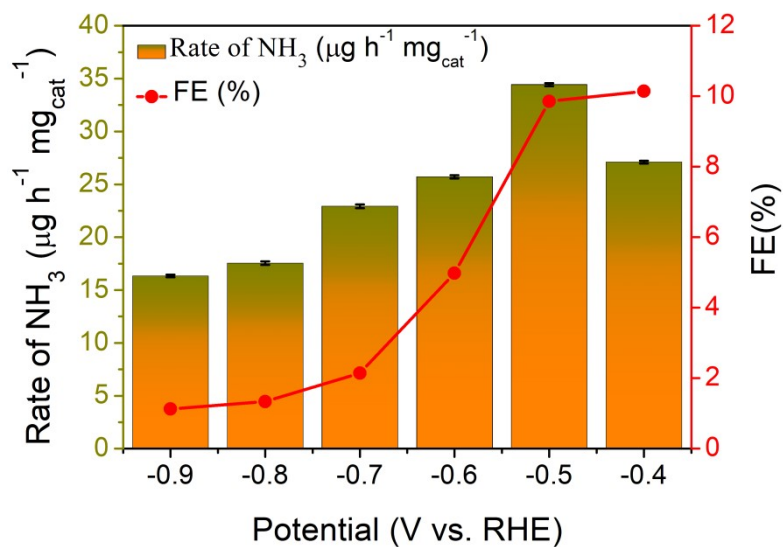


**Figure S19:** Ammonia yield rate and FE at different potentials for CoPc–MoS<sub>2</sub>.

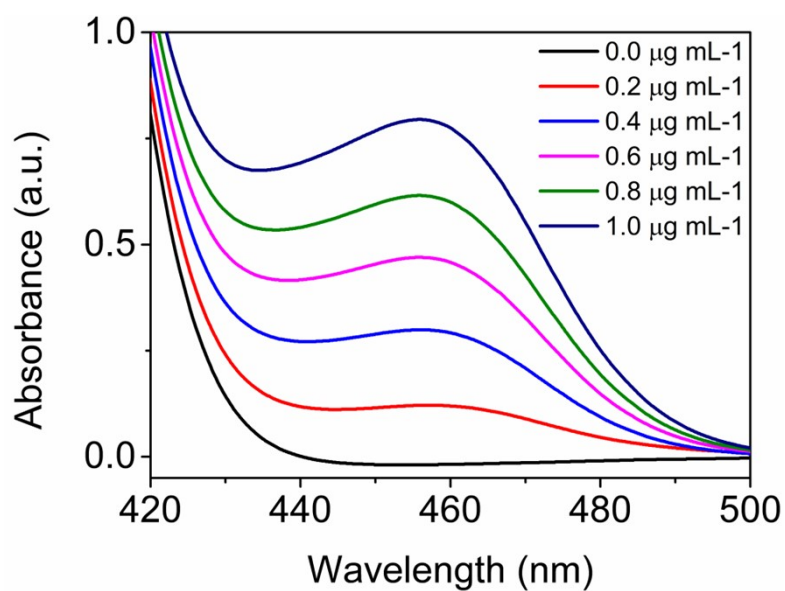


**Figure S20:** UV–vis absorption spectra of different N<sub>2</sub>H<sub>4</sub> concentrations

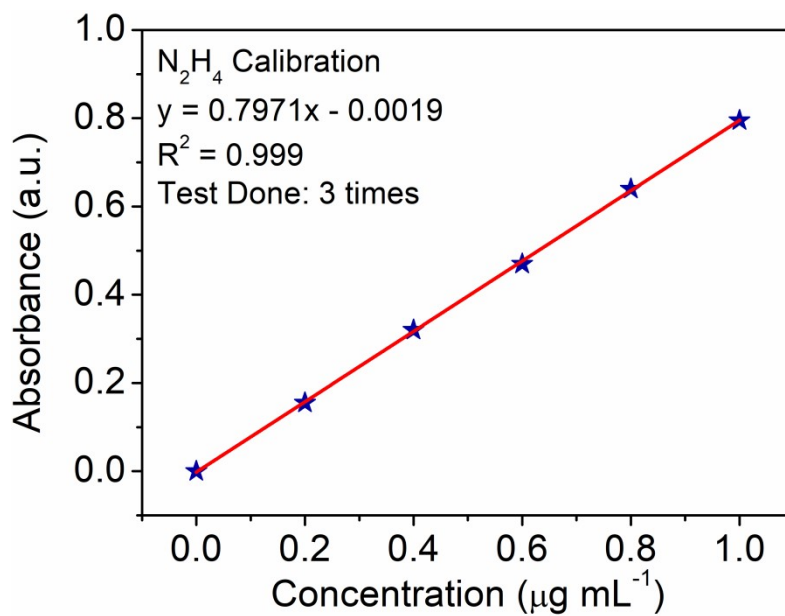


**Figure S21:** Calibration curve used for determination of N<sub>2</sub>H<sub>4</sub> concentration

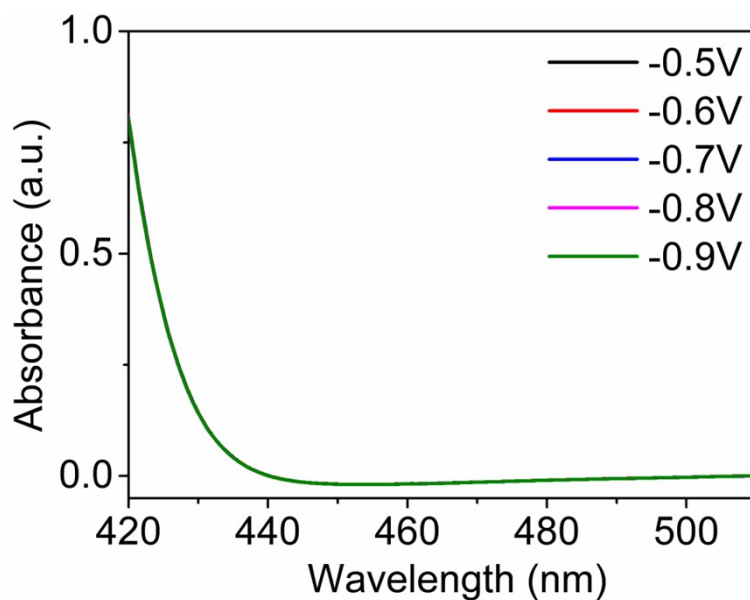


**Figure S22:** UV-vis absorption spectra for the formation of N<sub>2</sub>H<sub>4</sub> at different potentials

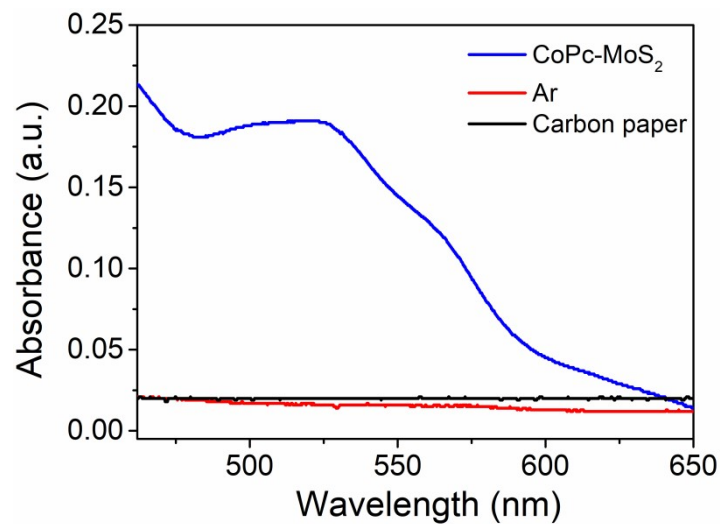


**Figure S23:** UV-vis absorption of the electrolytes of CoPc-MoS<sub>2</sub> at -0.6 V vs RHE in (N<sub>2</sub> + CO<sub>2</sub>) saturated, Ar saturated, and carbon paper in 0.1 M KHCO<sub>3</sub> solution

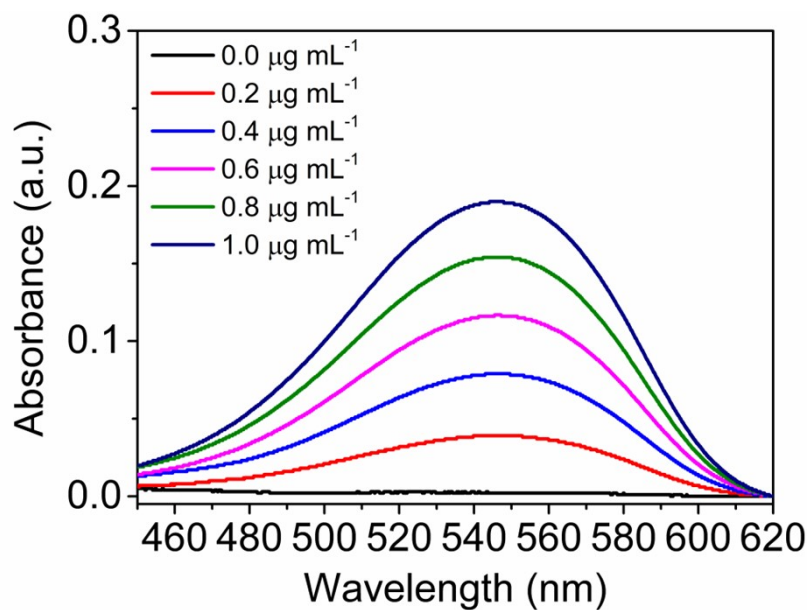


**Figure S24:** UV-vis absorption spectra of NO<sub>x</sub> of various concentration solutions

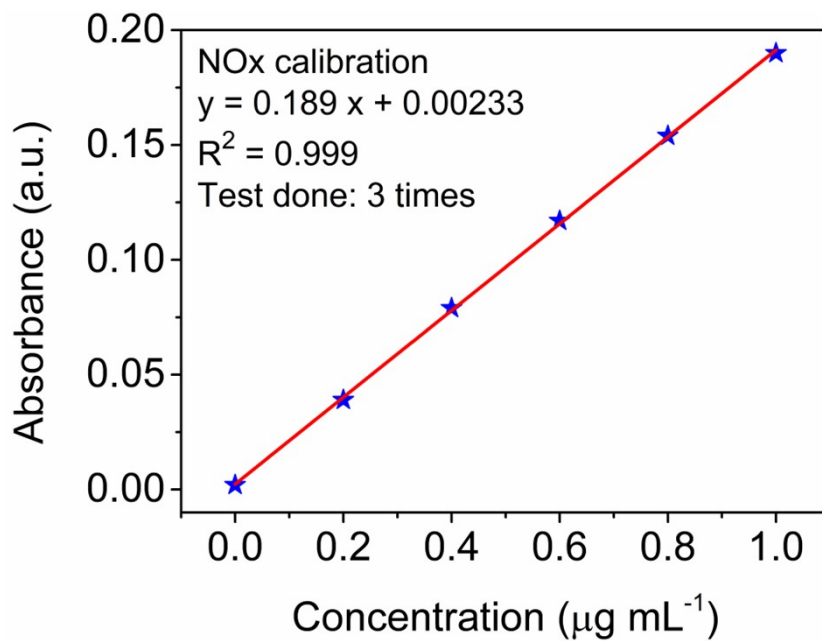


**Figure S25:** Calibration curve of NaNO<sub>2</sub> with the given concentrations

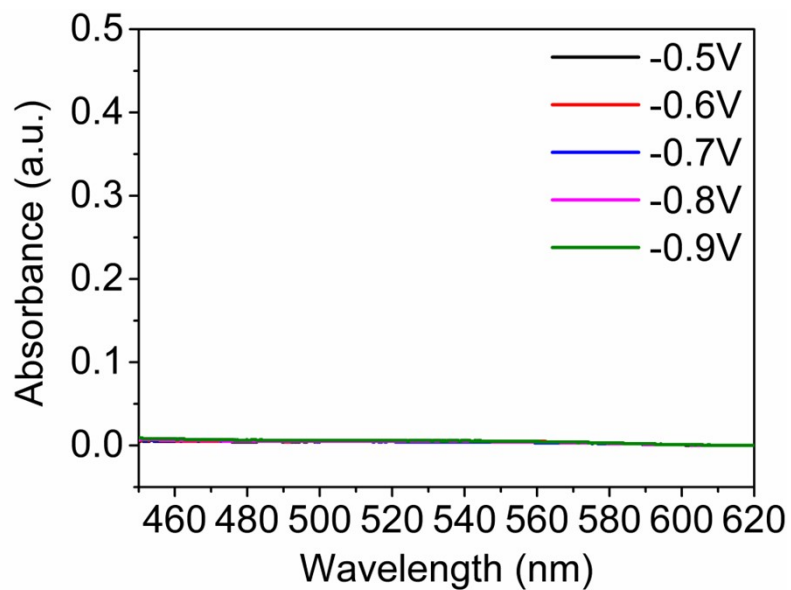


**Figure S26:** UV-vis absorption spectra for the formation of NO<sub>x</sub> at different potentials.

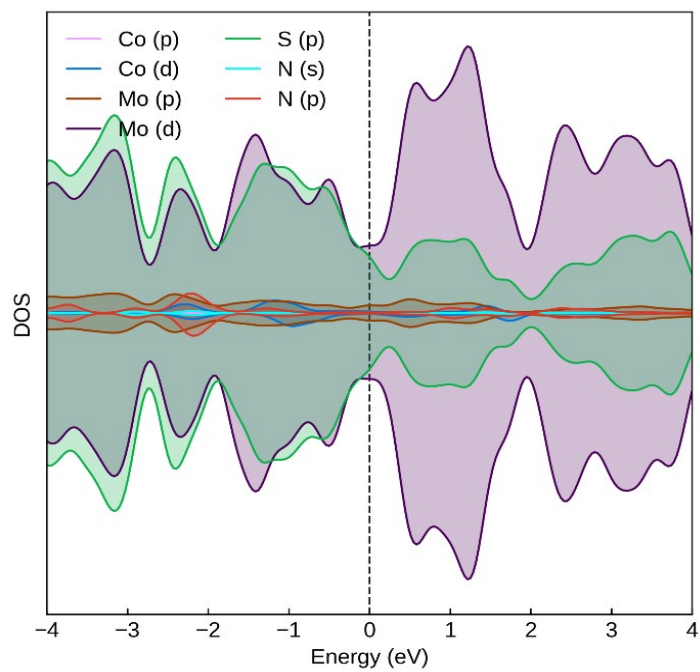


**Figure S27:** Partial DOS of the system where  $N_2$  adsorbed to both Co and Mo metal center. Shifted the VBM/Fermi level to 0 eV.

**Table S2: Comparison of the electrochemical urea performance for CoPc–MoS<sub>2</sub> with other electro-catalyst in solution media under ambient conditions.**

Electrocatalyst [Reference]	Electrolyte	Applied Potential (vs. RHE)	Nitrogen Source	Urea Yield Rate	FE (%)	Echem Cell
Pd <sub>1</sub> Cu <sub>1</sub> /TiO <sub>2</sub> [1]	0.1 M KHCO <sub>3</sub>	−0.4 V	N <sub>2</sub>	0.12 mmol g <sup>−1</sup> h <sup>−1</sup> 3.36 mmol g <sup>−1</sup> h <sup>−1</sup>	0.66 8.92	1. H–cell 2. Flow cell
CuPc [14]	0.1 M KHCO <sub>3</sub>	−0.6 V	N <sub>2</sub>	143.47 μg h <sup>−1</sup> mg <sup>−1</sup> <sub>cat</sub>	12.99	H–cell
BiFeO <sub>3</sub> /BiVO <sub>4</sub> [15]	0.1 M KHCO <sub>3</sub>	−0.4 V	N <sub>2</sub>	4.94 mmol h <sup>−1</sup> g <sup>−1</sup>	17.18	H–cell
Bi–BiVO <sub>4</sub> [16]	0.1 M KHCO <sub>3</sub>	−0.4 V	N <sub>2</sub>	5.91 mmol h <sup>−1</sup> g <sup>−1</sup>	12.55	H–cell
InOOH [17]	0.1 M KHCO <sub>3</sub>	−0.4 V	N <sub>2</sub>	6.85 mmol g <sup>−1</sup> h <sup>−1</sup>	20.97	H–cell
Ni <sub>3</sub> (BO <sub>3</sub> ) <sub>2</sub> [18]	0.1 M KHCO <sub>3</sub>	−0.5 V	N <sub>2</sub>	9.75 mmol g <sup>−1</sup> h <sup>−1</sup>	20.36	H–cell
MoP [19]	0.1 M KHCO <sub>3</sub>	−0.35 V	N <sub>2</sub>	12.4 μg h <sup>−1</sup> mg <sup>−1</sup>	36.5	H–cell
Fe–Ni pair [20]	0.1 M KHCO <sub>3</sub> + 50 mM KNO <sub>3</sub> or KNO <sub>2</sub>	−1.5 V	NO <sub>3</sub> <sup>−</sup>	20.2 mmol g <sup>−1</sup> h <sup>−1</sup>	17.8	H–cell
<b>CoPc–MoS<sub>2</sub> (This Work)</b>	<b>0.1 M KHCO<sub>3</sub></b>	<b>−0.7 V</b>	<b>N<sub>2</sub></b>	<b>175.6 μg h<sup>−1</sup> mg<sup>−1</sup><sub>cat</sub></b>	<b>15.12</b>	<b>H–cell</b>

**SI 34. References:**

[1] C. Chen, X. Zhu, X. Wen, Y. Zhou, L. Zhou, H. Li, L. Tao, Q. Li, S. Du, T. Liu, D.

- Yan, C. Xie, Y. Zou, Y. Wang, R. Chen, J. Huo, Y. Li, J. Cheng, H. Su, X. Zhao, W. Cheng, Q. Liu, H. Lin, J. Luo, J. Chen, M. Dong, K. Cheng, C. Li, S. Wang, *Nat. Chem.* 2020, **12**, 717.
- [2] G. W. Watt, J. D. Crisp, *Anal. Chem.* 1952, **24**, 2006.
- [3] G. Kresse, and D. Joubert, *Phys. Rev. B*, 1999, **59**, 1758.
- [4] G. Kresse, and J. Furthmuller, *Comp. Mat. Sci.*, 1996, **6**, 15–50.
- [5] G. Kresse, and J. Furthmuller, *Phys. Rev. B*, 1996, **54**, 11169–11186.
- [6] S. Grimme, J. Antony, S. Ehrlich, and H. Kreig, *J. Chem. Phys.*, 2010, **132**, 154104.
- [7] G. Henkelman, A. Arnaldsson, and H. Jonsson, *Comp. Mat. Sci.*, 2006, **36**, 354–360.
- [8] Y. Cheng, Y. Song, and Y. Zhang. *Phys. Chem. Chem. Phys.*, 2020, **22**, 6772-6782
- [9] W. Feng, L. Chen, M. Qin, X. Zhou, Q. Zhang, Y. Miao, K. Qiu, Y. Zhang, C. He, *Sci. Rep.* 2015, **5**, 1.
- [10] T. Liu, C. Wang, X. Gu, H. Gong, L. Cheng, X. Shi, L. Feng, B. Sun, Z. Liu, *Adv. Mater.* 2014, **26**, 3433–3440.
- [11] K.C. Lalithambika, K. Shanmugapriya, S. Sriram, *Appl. Phys. A* 2019, **125**, 817.
- [12] X. Ji, T. Zou, H. Gong, Q. Wu, Z. Qiao, W. Wu, H. Wang, *Cryst. Res. Technol.* 2016, **51**, 2, 154–159.
- [13] A. Kumar, S. Samanta, S. Latha, A.K. Debnath, A. Singh, K.P. Muthe, H.C. Barshilia, *RSC Adv.* 2017, **7**, 7, 4135–4143.
- [14] J. Mukherjee, S. Paul, A. Adalder, S. Kapse, R. Thapa, S. Mandal, B. Ghorai, S. Sarkar, U.K. Ghorai, *Adv. Funct. Mater.* 2022, **32**, 2200882.
- [15] M. Yuan, J. Chen, Y. Bai, Z. Liu, J. Zhang, T. Zhao, Q. Shi, S. Li, X. Wang and G. Zhang, *Chem. Sci.*, 2021, **12**, 6048–6058.
- [16] M. Yuan, J. Chen, Y. Bai, Z. Liu, J. Zhang, T. Zhao, Q. Wang, S. Li, H. He and G. Zhang, *Angew. Chemie - Int. Ed.*, 2021, **60**, 10910–10918.
- [17] M. Yuan, H. Zhang, Y. Xu, R. Liu, R. Wang, T. Zhao, J. Zhang, Z. Liu, H. He, C. Yang, S. Zhang and G. Zhang, *Chem Catal.*, 2022, **2**, 309–320.

- [18] M. Yuan, J. Chen, Y. Xu, R. Liu, T. Zhao, J. Zhang, Z. Ren, Z. Liu, C. Streb, H. He, C. Yang, S. Zhang and G. Zhang, *Energy Environ. Sci.*, 2021, **14**, 6605–6615.
- [19] D. Jiao, Y. Dong, X. Cui, Q. Cai, C.R. Cabrera, J. Zhao and Z. Chen, *J. Mater. Chem. A*, 2023,**11**, 232–240
- [20] X. Zhang, X. Zhu, S. Bo, C. Chen, M. Qiu, X. Wei, N. He, C. Xie, W. Chen, J. Zheng, P. Chen, S.P. Jiang, Y. Li, Q. Liu, and S. Wang, *Nat. Commun.* 2022, **13**, 5337.